ISME

www.nature.com/ismecomms

ARTICLE OPEN

A meta-analysis of the stony coral tissue loss disease microbiome finds key bacteria in unaffected and lesion tissue in diseased colonies

Stephanie M. Rosales[1,2✉], Lindsay K. Huebner[3], James S. Evans[4], Amy Apprill[5], Andrew C. Baker[6], Cynthia C. Becker[5], Anthony J. Bellantuono[7], Marilyn E. Brandt[8], Abigail S. Clark[9,10], Javier del Campo[11], Caroline E. Dennison[6], Katherine R. Eaton[1,2,12], Naomi E. Huntley[13], Christina A. Kellogg[4], Mónica Medina[13], Julie L. Meyer[14], Erinn M. Muller[12], Mauricio Rodriguez-Lanetty[7], Jennifer L. Salerno[15], William B. Schill[16], Erin N. Shilling[17], Julia Marie Stewart[13] and Joshua D. Voss[17]

Stony coral tissue loss disease (SCTLD) has been causing significant whole colony mortality on reefs in Florida and the Caribbean. The cause of SCTLD remains unknown, with the limited concurrence of SCTLD-associated bacteria among studies. We conducted a meta-analysis of 16S ribosomal RNA gene datasets generated by 16 field and laboratory SCTLD studies to find consistent bacteria associated with SCTLD across disease zones (vulnerable, endemic, and epidemic), coral species, coral compartments (mucus, tissue, and skeleton), and colony health states (apparently healthy colony tissue (AH), and unaffected (DU) and lesion (DL) tissue from diseased colonies). We also evaluated bacteria in seawater and sediment, which may be sources of SCTLD transmission. Although AH colonies in endemic and epidemic zones harbor bacteria associated with SCTLD lesions, and aquaria and field samples had distinct microbial compositions, there were still clear differences in the microbial composition among AH, DU, and DL in the combined dataset. Alpha-diversity between AH and DL was not different; however, DU showed increased alpha-diversity compared to AH, indicating that, prior to lesion formation, corals may undergo a disturbance to the microbiome. This disturbance may be driven by Flavobacteriales, which were especially enriched in DU. In DL, Rhodobacterales and Peptostreptococcales–Tissierellales were prominent in structuring microbial interactions. We also predict an enrichment of an alpha-toxin in DL samples which is typically found in Clostridia. We provide a consensus of SCTLD-associated bacteria prior to and during lesion formation and identify how these taxa vary across studies, coral species, coral compartments, seawater, and sediment.

ISME Communications; https://doi.org/10.1038/s43705-023-00220-0

INTRODUCTION

Stony coral tissue loss disease (SCTLD) causes focal or multifocal lesions on hard coral colonies (order Scleractinia) leading to exposed skeleton from tissue loss [1, 2]. Affected colony mortality rates can be as high as 99%, but survival is highly dependent on the coral species [3]. While some corals, such as branching Caribbean acroporids, are not impacted by this disease [3], SCTLD nevertheless has a wide host range, affecting over half of Caribbean coral species (~22 species) [2, 3]. This has resulted in a decline in coral species richness, coral cover, and ecosystem function throughout Florida and the Caribbean [3–10].

The cause of SCTLD is currently unknown, but multiple hypotheses of the potential etiology have been proposed, including abiotic stressors [3, 4, 11, 12], viruses [13, 14], bacteria [15, 16], or a combination of these factors. SCTLD was first detected in September 2014 off the coast of Miami, Florida, which coincided with a coral bleaching event and a dredging project to expand the Miami Port [3, 4]. This led to speculation that heat stress and/or sedimentation may be linked to SCTLD. Evidence to date suggests that thermal stress has either no association with SCTLD [17] or slows disease progression [18], but sediments may contribute to SCTLD transmission [11, 12].

[1]The University of Miami, Cooperative Institute for Marine and Atmospheric Studies, Miami, FL, USA. [2]National Oceanic and Atmospheric Administration, Atlantic Oceanographic and Meteorological Laboratory, Miami, FL, USA. [3]Florida Fish and Wildlife Conservation Commission, Fish and Wildlife Research Institute, St. Petersburg, FL, USA. [4]U.S. Geological Survey, St. Petersburg Coastal and Marine Science Center, St. Petersburg, FL, USA. [5]Woods Hole Oceanographic Institution, Marine Chemistry and Geochemistry, Woods Hole, MA, USA. [6]The University of Miami, Rosenstiel School of Marine, Atmospheric, and Earth Science, Department of Marine Biology and Ecology, Miami, FL, USA. [7]Florida International University, Department of Biological Sciences, Miami, FL, USA. [8]The University of the Virgin Islands, Center for Marine and Environmental Studies, St. Thomas, VI, USA. [9]The College of the Florida Keys, Marine Science and Technology, Key West, FL, USA. [10]Elizabeth Moore International Center for Coral Reef Research and Restoration, Mote Marine Laboratory, Summerland Key, FL, USA. [11]Institut de Biologia Evolutiva (CSIC - Universitat Pompeu Fabra)-Barcelona, Barcelona, Spain. [12]Mote Marine Laboratory, Coral Health and Disease Program, Sarasota, FL, USA. [13]The Pennsylvania State University, Biology Department, University Park, PA, USA. [14]University of Florida, Soil, Water, and Ecosystem Sciences Department, Gainesville, FL, USA. [15]George Mason University, Potomac Environmental Research and Education Center, Department of Environmental Science and Policy, Woodbridge, VA, USA. [16]U.S. Geological Survey, Eastern Ecological Science Center, Leetown, WV, USA. [17]Harbor Branch Oceanographic Institute, Florida Atlantic University, Fort Pierce, FL, USA. ✉email: Stephanie.Rosales@noaa.gov

Received: 23 September 2022 Revised: 24 January 2023 Accepted: 8 February 2023
Published online: 09 March 2023

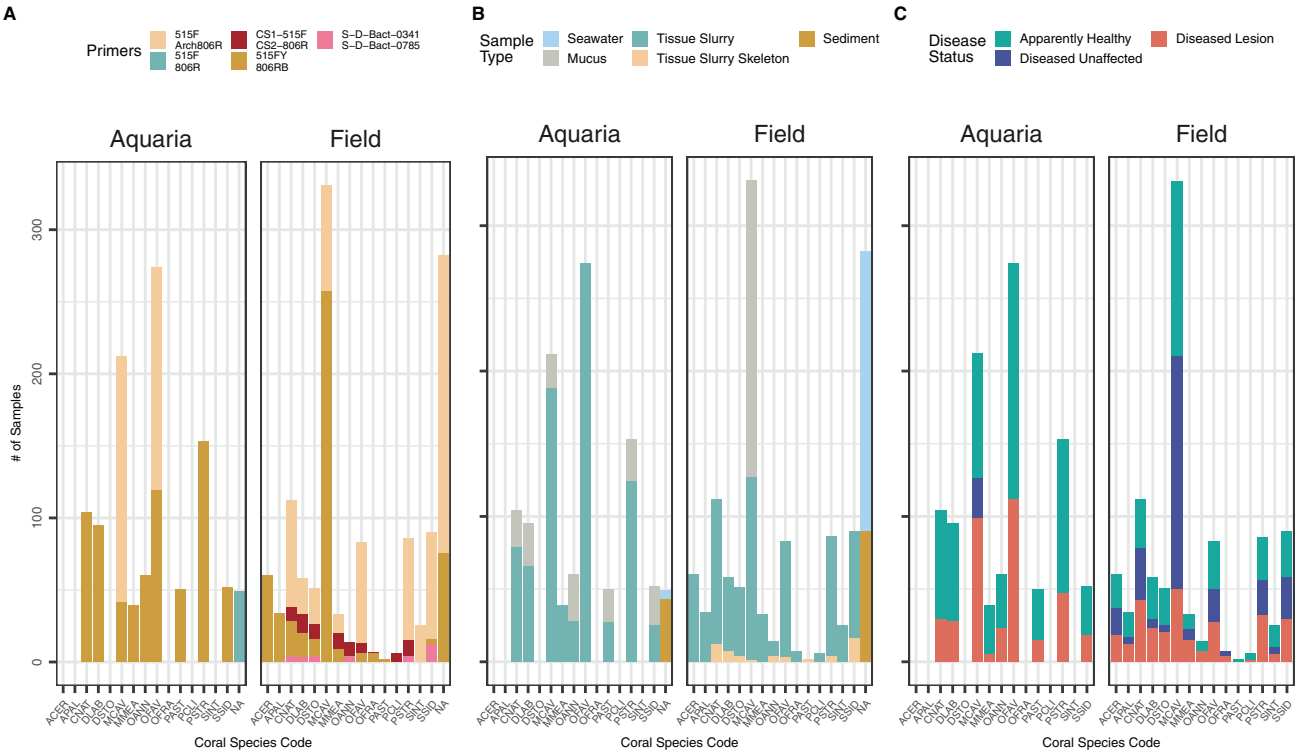

Fig. 1 The number of aquaria and field samples for each coral species. A small subunit (SSU) rRNA gene primer sets, **B** sample type, and **C** disease state. NAs in (**A**, **B**) represent sediment and seawater samples. Coral species codes represent the following: *Acropora cervicornis* (ACER), *Acropora palmata* (APAL), *Colpophyllia natans* (CNAT), *Diploria labyrinthiformis* (DLAB), *Dichocoenia stokesii* (DSTO), *Montastraea cavernosa* (MCAV), *Meandrina meandrites* (MMEA), *Orbicella annularis* (OANN), *Orbicella faveolata* (OFAV), *Orbicella franksi* (OFRA), *Porites astreoides* (PAST), *Pseudodiploria clivosa* (PCLI), *Pseudodiploria strigosa* (PSTR), *Stephanocoenia intersepta* (SINT), and *Siderastrea siderea* (SSID).

SCTLD is contagious and can be transmitted through the water column [18–20] or through direct coral-coral contact [21], suggesting that it is caused by a biotic source(s) [9, 19]. Viruses have been found in SCTLD-affected corals, although similar virus morphologies and sequences were also detected in apparently healthy corals at similar abundances [13, 14]. Studies have also detected ciliates [1, 19, 22] and endolithic organisms [1] associated with SCTLD, but other eukaryotes have not been linked with this disease.

The most well-studied SCTLD microbial group is the bacterial community, which has mostly been examined using small subunit (SSU) 16S rRNA gene analysis [11, 12, 15, 16, 22–27]. It is likely that the bacterial community is important for SCTLD progression, since there is a shift in bacterial composition from healthy corals to diseased corals, and antibiotics can mitigate SCTLD lesion progression [19, 28, 29]. Orders such as Rhodobacterales, Rhizobiales, Clostridiales, Alteromonadales, and Vibrionales have been described across many studies, but there have been discrepancies, especially at finer taxonomic levels. Further, a consensus on the key bacteria correlated with SCTLD across locations and coral species remains a topic of discussion.

The lack of consensus across studies may be due to biological factors such as coral species-specific microbiomes, the environment in which samples were collected, or other biological variables. However, variability across studies may also arise from different laboratory processing, library preparation, and analytical approaches [30]. In addition, results are often reported at different taxonomic levels such as order [11], family [16], genus [15], and species [23], which can make it difficult to compare across studies. Thus, to better understand SCTLD, a meta-analysis of available SSU 16S rRNA datasets can reduce biases associated with pipelines and reporting strategies. In this study, we examined microbiome datasets from 16 SCTLD studies using a consistent analysis pipeline to determine global patterns and taxa associated with SCTLD.

RESULTS

Summary of SCTLD microbiome studies

Initially, datasets were acquired from 17 SCTLD studies, but one study [24] did not pass quality filtering and was removed from the analysis, resulting in 16 SCTLD studies used in this meta-analysis. In addition, one *Acropora* spp. rapid tissue loss (RTL) disease study was included for comparison of bacteria which may be associated more generally with coral tissue loss diseases (Supplementary Table 1). The combined dataset included 2425 samples, representing various coral species and environments described below. A total of 63 miscellaneous samples such as lab controls were included in this total (Supplementary Table 1). Samples from the studies were sequenced using five primer pairs: CS1-515F/CS2-806R [31] with additional 5′ linker sequences [32] ($n = 79$), 515FY [33]/806RB [34] ($n = 1219$), S-D-Bact-0341-b-S-17/S-D-Bact-0785-a-A-21 [35] ($n = 31$), 515F/806R [31] ($n = 49$), and 515F [31]/Arch806R [36] ($n = 984$; Fig. 1A). Although five primer pairs were used across studies, only the forward reads were evaluated in this analysis (see "Methods"). A description of the differences between 515F primers can be found in detail [34].

Samples were collected throughout Florida and the U.S. Virgin Islands (USVI). Field samples totaled 1274, representing 40 sites, and a further 1088 samples were from aquaria (i.e., laboratory-based experiments; Fig. 1). Thirteen SCTLD-susceptible coral species were included, with *Montastraea cavernosa* (MCAV; $n = 543$) and *Orbicella faveolata* (OFAV; $n = 357$) most represented and *Pseudodiploria clivosa* (PCLI; $n = 6$) and *Orbicella franksi*

(OFRA; $n = 7$) least represented (Fig. 1). Coral samples ($n = 2031$) were from three compartments: mucus only ($n = 393$), mucus and surface tissue (tissue slurry; $n = 1585$), and skeleton samples with embedded coral tissue (tissue slurry skeleton; $n = 53$). Seawater ($n = 198$) and sediment ($n = 133$) samples from both the field and aquaria experiments also were included to evaluate potential sources of transmission of disease-associated bacteria (Fig. 1B). For seawater from aquaria experiments, 18 L samples were collected [27], while in the field between 60 mL and 1 L samples were collected [11, 25]. In sediment aquaria experiments, 2 mL samples were collected [12], and in the field, approximately 5 mL samples were collected (of the 5 mL, DNA was extracted from 0.25 g sediment [11]). Coral samples represented three SCTLD health states: apparently healthy colonies (AH), which was the most represented ($n = 1021$), followed by lesions on diseased colonies (DL; $n = 661$), and unaffected areas on diseased colonies (DU; $n = 349$; Fig. 1C). AH represents grossly normal tissue, DU grossly normal tissue on diseased colonies, and DL grossly abnormal tissue.

Differences in the microbial composition were found in AH corals among zones (vulnerable, endemic, and epidemic)

Differences in alpha-diversity were tested among three SCTLD zones: vulnerable (i.e., locations where the disease had not been observed/reported), endemic (i.e., locations where a disease outbreak had moved through the reef and no or few colonies had active lesions), and epidemic (i.e., locations where the outbreak was active and prevalent). For alpha-diversity, for AH field-sourced samples, after filtering, 41,504 amplicon sequence variants (ASVs) remained, which were reduced to 15,021 following rarefaction. Among the filtered AH samples, Shannon (alpha) diversity from the vulnerable zone was slightly higher (estimated marginal means (emmean) = 3.95) compared to the epidemic zone (emmean = 3.70), but this was not significant (Supplementary Fig. 1). For beta-diversity, both within and between-group differences were tested using a filtered counts table. Within-group beta-diversity (variation in microbial composition or dispersion) was not different between zones, but was significant for all comparisons between zones (PERMANOVA, *P*-adjusted (*P*adj) <0.03; Fig. 2A). Differential abundance analysis found 61 ASVs enriched between vulnerable and endemic sites (Fig. 2B, Supplementary Fig. 2, and Supplementary Table 2). In the endemic zone, the orders Synechococcales (*Cyanobium* PCC-6307; log-fold = 12.67) and an uncultured Flavobacteriales (log-fold = 9.96) contained ASVs with the highest log-fold change, but the order Flavobacteriales was the group of bacteria with the most enriched ASVs ($n = 13$), followed by SAR11 clade ($n = 4$) and Rhodobacterales ($n = 3$). Fewer ASVs were enriched between the vulnerable and epidemic zones ($n = 31$; Fig. 2C and Supplementary Table 3), with the highest log-fold ASV changes found in the orders Burkholderiales (*Delftia*; log-fold = 5.84) and Peptostreptococcales–Tissierellales (*Fusibacter*; log-fold = 5.65). Like in endemic sites, Flavobacteriales was the group with the most enriched ASVs in the epidemic zone ($n = 5$) and were detected in the three disease states (AH, DU, and DL; Supplementary Fig. 2).

Biome had the highest correlation to bacterial beta-diversity

Microbial dispersion at the ASV level was found to be different across primers, study, biome, year, all coral species, and sample type (Permutest: $P < 0.01$; Fig. 3). A PERMANOVA test for differences between microbial composition at the ASV level was also significant across all factors, with coral species having the highest correlation ($R^2 = 0.21$; Fig. 3E) and disease state showing the lowest correlation ($R^2 = 0.04$). Biome (i.e., aquaria and field) had the largest correlation to principal component 1 (PC1, R2 = 0.73; Supplementary Fig. 3) compared to other tested metadata factors, and showed a distinct separation when visualized (Fig. 3C). This was also evident even in sediment and seawater samples that were collected in aquaria studies, which clustered with coral samples from aquaria studies and not with field sediment and seawater samples. Given this pattern, SCTLD-affected corals (with the removal of *Acropora* spp.) were first combined (i.e., both aquaria and field) and analyzed. In subsequent analyses, the SCTLD-affected corals were divided by biome to identify potential differences between the two.

Bacterial communities differ across disease states, but this may depend upon the biome

When both biomes were combined (Fig. 4A), DL microbial communities were the most highly dispersed compared to both AH and DU (*P*adj < 0.01 each), but AH and DU were not different. Pairwise PERMANOVA was significant for all comparisons (*P*adj < 0.001 each; Fig. 4A). Among aquaria samples (Fig. 4B), the dispersion was lower in DU vs both DL (*P*adj < 0.01) and AH (*P*adj < 0.005), and was also dissimilar in AH vs DL (*P*adj = 0.0015). Like the combined samples, all aquaria samples were different in the pairwise PERMANOVA (*P*adj < 0.001 each; Fig. 4B). In field samples (Fig. 4C), the dispersion was only different between DL and AH. All pairwise PERMANOVA comparisons were significant in the field samples: AH vs DU (*P*adj < 0.02), AH vs DL (*P*adj < 0.01), and DU vs DL (*P*adj < 0.03; Fig. 4C).

Samples were also evaluated for alpha-diversity by disease state in each biome. After quality filtering and rarefaction across disease states, 39,513 ASVs remained. For aquaria and field samples combined, pairwise comparisons showed differences in Shannon diversity for AH vs DU and DL vs DU (*P*adj < 0.0001 each) but not AH vs DL, with mean alpha-diversity lowest in DL (emmean = 3.42) and highest in DU (emmean = 3.85; Supplementary Fig. 4A). In aquaria samples only, there were no differences in Shannon diversity by disease state, likely due to the low sample size of DU ($n = 27$, Supplementary Fig. 4B). In field samples, only DU vs DL was different (*P*adj < 0.01) with DU also showing the highest mean (emmean = 3.90) and DL the lowest (emmean = 3.63; Supplementary Fig. 4C) alpha-diversity.

When comparing differences in mean relative microbial abundances within disease states across biomes, AH samples differed between aquaria and field (Supplementary Fig. 4D): the orders Rhodobacterales (14.20 ± 5.2%) and Cytophagales (9.02 ± 12.32%) were dominant in aquaria samples, but in field samples, the dominant orders were Flavobacteriales (5.75 ± 2.15%) and Synechococcales (3.77 ± 5.88%). Like AH aquaria samples, DU aquaria samples had the highest mean relative abundances in Rhodobacterales, but at a much lower percentage (1.06 ± 3.81%). The DU field samples were also similar to their AH counterparts, showing the highest relative abundances in Flavobacteriales (6.43 ± 1.89%) and Synechococcales (4.45 ± 6.26%). In the DL samples, both aquaria and field samples were dominated by Rhodobacterales, but the aquaria samples had a higher relative abundance of Rhodobacterales (15.34 ± 6.84%) than samples from the field (6.61 ± 4.12%). As with aquaria AH samples, Cytophagales (3.28 ± 11.22%) were also the second most relatively abundant order in DL aquaria samples but were not dominant in field DL samples. Peptostreptococcales–Tissierellales was a dominant DL member at similar mean relative abundances in both aquaria (3.21 ± 6.40%) and field samples (3.79 ± 9.06%; Supplementary Fig. 4D).

Indicator taxa were detected across sample types and zones

The combined three coral compartments (mucus, tissue slurry, and tissue slurry skeleton), from both field and aquaria, yielded a total of 109 differentially abundant ASVs between AH vs DU (Fig. 5A, Supplementary Fig. 5A, and Supplementary Table 4). DU mucus samples showed the highest log-fold change compared to AH in the orders Flavobacteriales (NS5 marine group; log-fold = 6.33) and Synechococcales (*Cyanobium* PCC-6307; log-fold = 6.19), with Flavobacteriales having the most enriched ASVs ($n = 9$). Similarly,

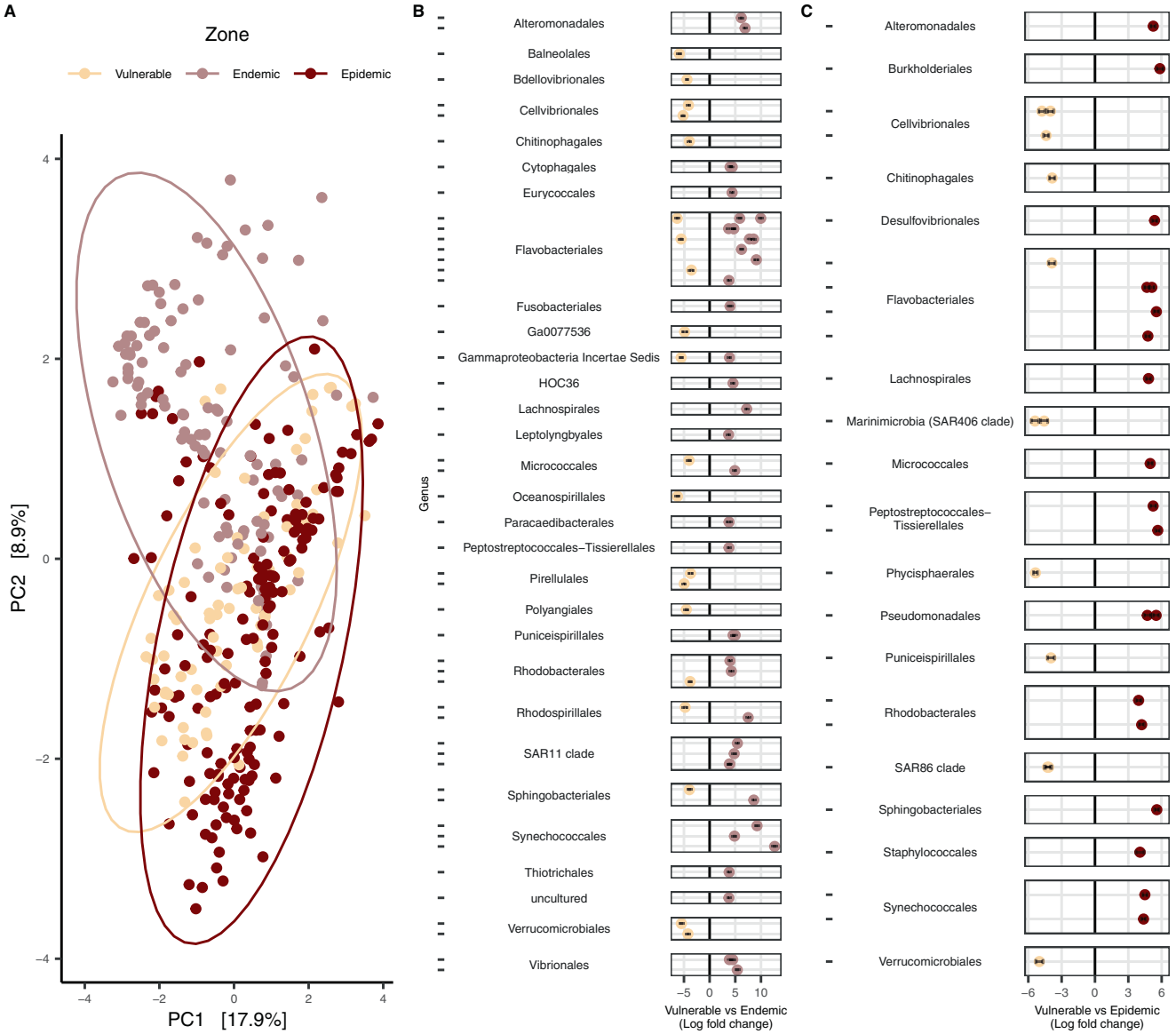

Fig. 2 Comparisons among microbial communities of field-sourced apparently healthy (AH) coral colonies across stony coral tissue loss disease (SCTLD) zones (vulnerable, endemic, and epidemic). A beta-diversity (centered log-ratio transformed and plotted with a Euclidean distance), and differential abundance analysis in (**B**) vulnerable vs endemic zones, and **C** vulnerable vs epidemic zones. ASVs are grouped by genus (represented by dashes) on the y axis and then by order, and only ASVs with a *P*adj < 0.001, a W statistic >90, and a log-fold change < −2 and >2 were visualized. AH samples from the three coral compartments (mucus, tissue slurry, and tissue slurry skeleton) were included and *Acropora* spp. samples were excluded from the analysis. The ellipses in (**A**) represent the center of the Euclidean distance from the respective zone with a 95% confidence of the ellipses.

DU tissue slurry samples were most enriched in Synechococcales (*Synechococcus* CC9902; log-fold = 20.04) and Flavobacteriales (NS5 marine group; log-fold = 12.71), with Flavobacteriales having the most enriched ASVs ($n = 9$). Tissue slurry skeleton sample comparisons of AH vs DU identified no ASVs enriched in DU. In addition to coral compartment samples, ASVs enriched in AH and DU samples were also present within sediment and seawater samples. The enriched taxa were also detected across the three zones with Flavobacteriales and Synechococcales found at higher relative abundances in sediment and seawater of endemic and epidemic zones compared to the vulnerable zone (Supplementary Fig. 5). However, some taxa such as Burkholderiales and Staphylococcales were also present at high relative abundances in lab control samples compared to other taxa and thus could be artifacts of contamination (Fig. 5B) [37].

The three combined coral compartments yielded fewer differentially abundant ASVs in AH vs DL ($n = 79$; Fig. 6A, Supplementary Fig. 6, and Supplementary Table 5) compared to AH vs DU (Fig. 5A). In DL mucus samples, ASVs from the orders Desulfovibrionales (*Halodesulfovibrio*; log-fold = 13.96) and Rhodobacterales (*Shimia*; log-fold = 13.18) were the most enriched, and Rhodobacterales had the most enriched ASVs overall ($n = 8$). In DL tissue slurries, the ASVs with the highest enrichment were two Rhodobacterales from an uncharacterized genus (log-fold = 15.77) and one from the genus *Tropicibacter* (log-fold = 13.46). Rhodobacterales were also the order with the most enriched ASVs in DL compared with AH tissue slurries ($n = 14$), followed by Peptostreptococcales–Tissierellales ($n = 6$). Among tissue slurry skeleton samples, only one ASV was enriched in DL (Burkholderiales, *Achromobacter*; log-fold = 1.49), but just like in DU samples,

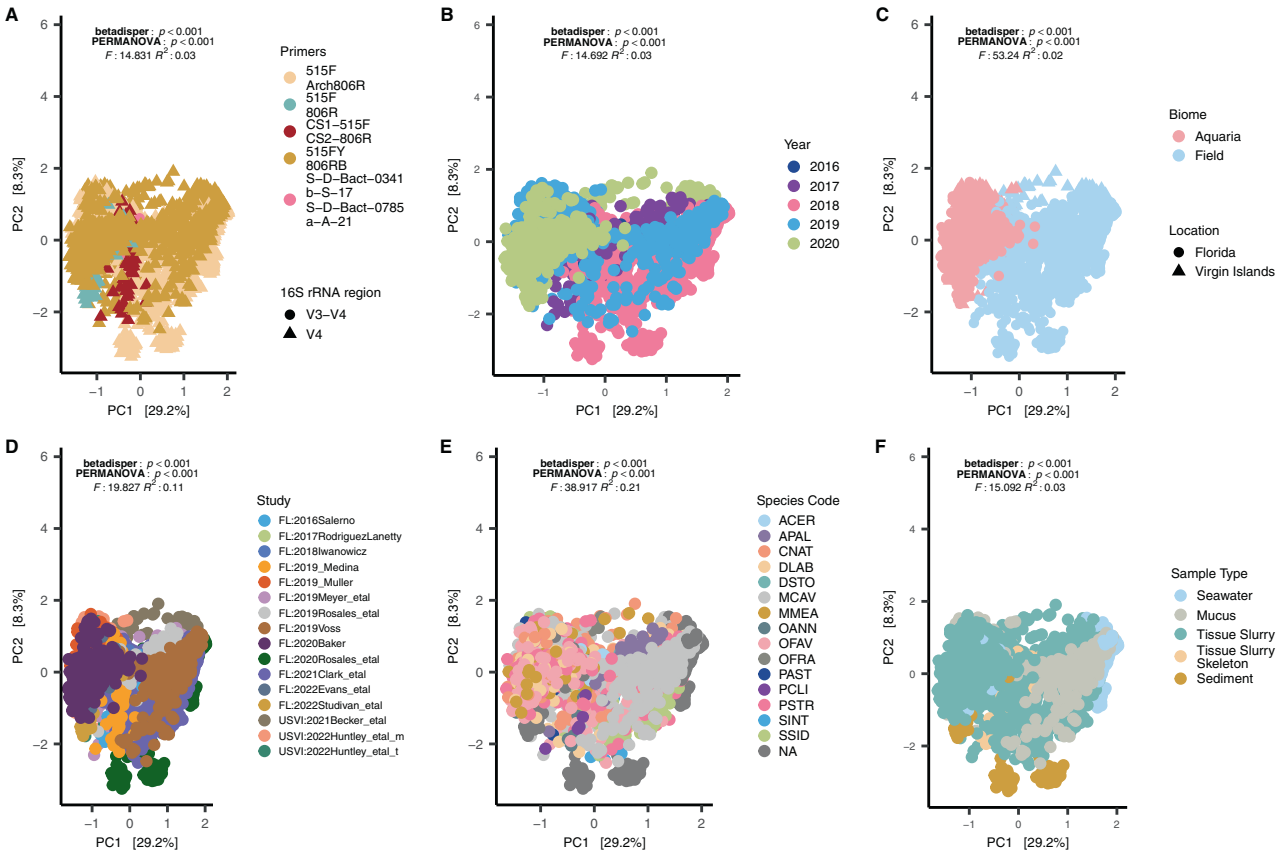

Fig. 3 Microbial beta-diversity of all coral species (stony coral tissue loss disease [SCTLD]-susceptible corals and *Acropora* spp.) and sample types (coral, sediment, and seawater) show differences within and between microbial communities. A small subunit (SSU) 16S rRNA gene primers, **B** year, **C** biome, **D** study, **E** coral species, and **F** sample type. All plots were centered log-ratio transformed and visualized with a Euclidean distance. The NAs in (**E**) represent sediment and seawater samples; coral species codes are defined in Fig. 1 legend.

Burkholderiales was found at high relative abundances in lab controls and therefore could be a laboratory artifact (Fig. 6B). ASVs enriched in DL were also found in sediment and seawater (Fig. 6B and Supplementary Fig. 6); however, Rhodobacterales was commonly and abundantly found in the vulnerable zone, while Peptostreptococcales–Tissierellales was absent or found at low relative abundances (Supplementary Fig. 6).

When OFAV and MCAV (the most-sampled coral species) were removed from the analysis, similar patterns were still identified in beta-diversity (Supplementary Fig. 7A) and differential abundance when compared to the analysis of all SCTLD-susceptible species. For DU, 18 (35.3%) ASVs were shared between the two analyses (i.e., with vs without OFAV and MCAV), but more unique ASVs were found enriched in the analysis without OFAV and MCAV compared to the analysis that included all SCTLD-susceptible corals (Supplementary Fig. 7B). Still, the two analyses shared more enriched bacterial families/orders compared to the number that was enriched only within each individual analysis. In DL, the differential abundance analysis without OFAV and MCAV compared to that with all SCTLD-susceptible coral species showed that the majority of enriched ASVs were shared ($n = 25$; 39.1%) between the two analyses (Supplementary Fig. 7C).

Indicator taxa presence varied across coral species and studies

Six coral species were represented by a high number of samples ($n > 76$ samples each), and all ASVs only enriched in DU were found within all of those species. The seven coral species with lower sampling frequencies ($n < 76$ each) varied in the numbers of DU-enriched ASVs present (Supplementary Fig. 8A). For example, *Dichocoenia stokesii* (DSTO) contained all DU-enriched taxa, and *Stephanocoenia intersepta* (SINT) had all genera present but one, which belonged to Flavobacteriales. In comparison, *Pseudodiploria clivosa* (PCLI) had the fewest DU-enriched taxa ($n = 3$) among the coral species. Four orders were not present in *Acropora* spp. samples and included: Blastocatellales, Pirellulales, Sphingobacteriales, and Peptostreptococcales–Tissierellales. Across studies, the order Sphingobacteriales was not found in any aquaria study but was found in 50% of field studies (Supplementary Fig. 8B). In addition, no aquaria study had representatives from all DU-enriched taxa, likely because of low DU samples in aquaria, but four field studies had all taxa. The two studies with the fewest representatives were studies that used V3–V4 primers (Supplementary Table 1).

The ASVs enriched only in DL were also present in all high-frequency coral species, while none of the low-frequency coral species had all of the DL-enriched taxa (Supplementary Fig. 9A). PCLI possessed the fewest DL-enriched genera ($n = 9$) followed by *Orbicella franksi* (OFRA; $n = 15$). More DL-enriched orders ($n = 11$) were absent from *Acropora* spp. corals than DU-enriched orders ($n = 4$); the DL orders not present in *Acropora* were: Bacteroidales, Beggiatoales, Burkholderiales, Cellvibrionales, Clostridiales, Desulfovibrionales, Oligoflexales, Peptostreptococcales–Tissierellales, Rhizobiales, Thiotrichales, and Verrucomicrobiales. Across studies, three had all the DL-enriched orders (all aquaria studies), and the fewest orders were present in those which used V3–V4 primers (Supplementary Fig. 9B), as with the DU-enriched orders.

Alphaproteobacteria and Clostridia were found associated with SCTLD bacterial community interactions

In a network analysis of co-associated ASVs, a total of nine modules were identified, with two that were significantly and

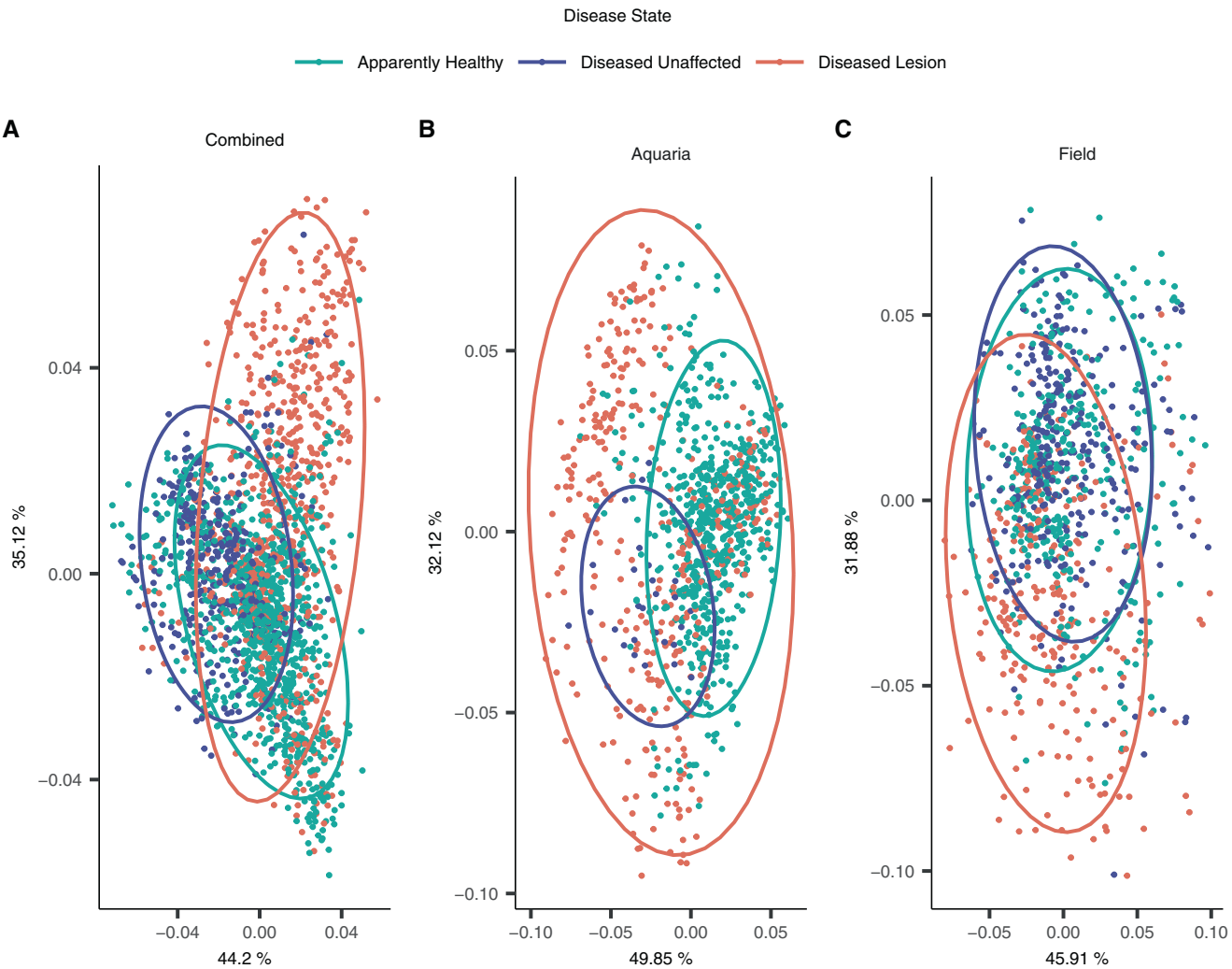

Fig. 4 Microbial differences in coral disease state among apparently healthy colonies (AH), and unaffected (DU) and lesion (DL) areas on diseased colonies in beta-diversity using a robust Aitchison Distance. A both aquaria and field samples ("Combined"), and **B** aquaria and **C** field samples only. Samples from *Acropora* spp. were excluded and the three coral compartments (mucus, tissue slurry, and tissue slurry skeleton) were included in this analysis. The ellipses represent the center of the Euclidean distance from the respective disease state with a 95% confidence of the ellipses.

positively correlated to AH ($R^2 = 0.1$ and 0.26), three to DU ($R^2 = 0.12$, 0.31, and 0.46), and four to DL ($R^2 = 0.17$, 0.22, 0.46, and 0.47; Supplementary Fig. 10). The modules with the highest positive correlation to each disease state had 134 (AH; blue), 158 (DU; green), and 146 (DL; pink) co-abundant ASVs (Supplementary Fig. 10) and were used for undirected network analysis (Fig. 7). Although AH had the second largest module, the network was smaller than both DU and DL, with only 56 ASV nodes and 59 edges (connections between nodes). DU had the largest network, with 138 nodes and 293 edges, followed by DL, with 123 nodes and 204 edges. In AH, the node with the most neighbors ($n = 7$) was from the class Polyangia (order Polyangiales), which was also considered a key player (i.e., provides cohesiveness, connectedness, and is embedded in a network [38]; Fig. 7) in the AH network. The two nodes with the highest correlation to the blue weighted correlation network analysis (WGCNA) module (Supplementary Fig. 10) were from the class Bacteroidia (Chitinophagales; $R^2 = 0.88$ and 0.87).

In the DU network, highly connected nodes included three orders from the class Alphaproteobacteria (SAR11 clade ($n = 16$), Rhodobacterales ($n = 11$), and Rhodospirillales ($n = 11$); Fig. 7). Alphaproteobacteria were among the classes assigned as key players, but additional key players included: Cyanobacteria, Bacteroidia, and Polyangia. The nodes most highly correlated to their respective WGCNA modules were SAR86 clade ($R^2 = 0.88$) and Rhodospirillales ($R^2 = 0.88$).

The DL network had nodes with the most neighbors compared to AH and DU and was driven by Alphaproteobacteria (two Rhodobacterales nodes ($n = 22$ and $n = 16$), and Rhizobiales ($n = 9$)), and Bacteroidia (Flavobacteriales ($n = 12$); Fig. 7). While Alphaproteobacteria (Rhodobacterales and Rhizobiales) were found as key players in DL, Flavobacteriales were not. Additional key players in DL included Clostridia, Chlamydiae, and Campylobacteria. The class Clostridia had the highest correlations to the DL pink WGCNA module (Peptostreptococcales–Tissierellales; $R^2 = 0.77$ and Lachnospirales $R^2 = 0.76$; Supplementary Fig. 10). The most prevalent classes in DL networks were Alphaproteobacteria ($n = 39$; mainly Rhodobacterales, $n = 29$) and Clostridia ($n = 23$; mainly Peptostreptococcales–Tissierellales, $n = 13$).

The top microbial functional pathways were more enriched in DL compared to AH and DU

To identify differences in the potential microbial function between disease states, we used the SSU 16S rRNA gene for functional

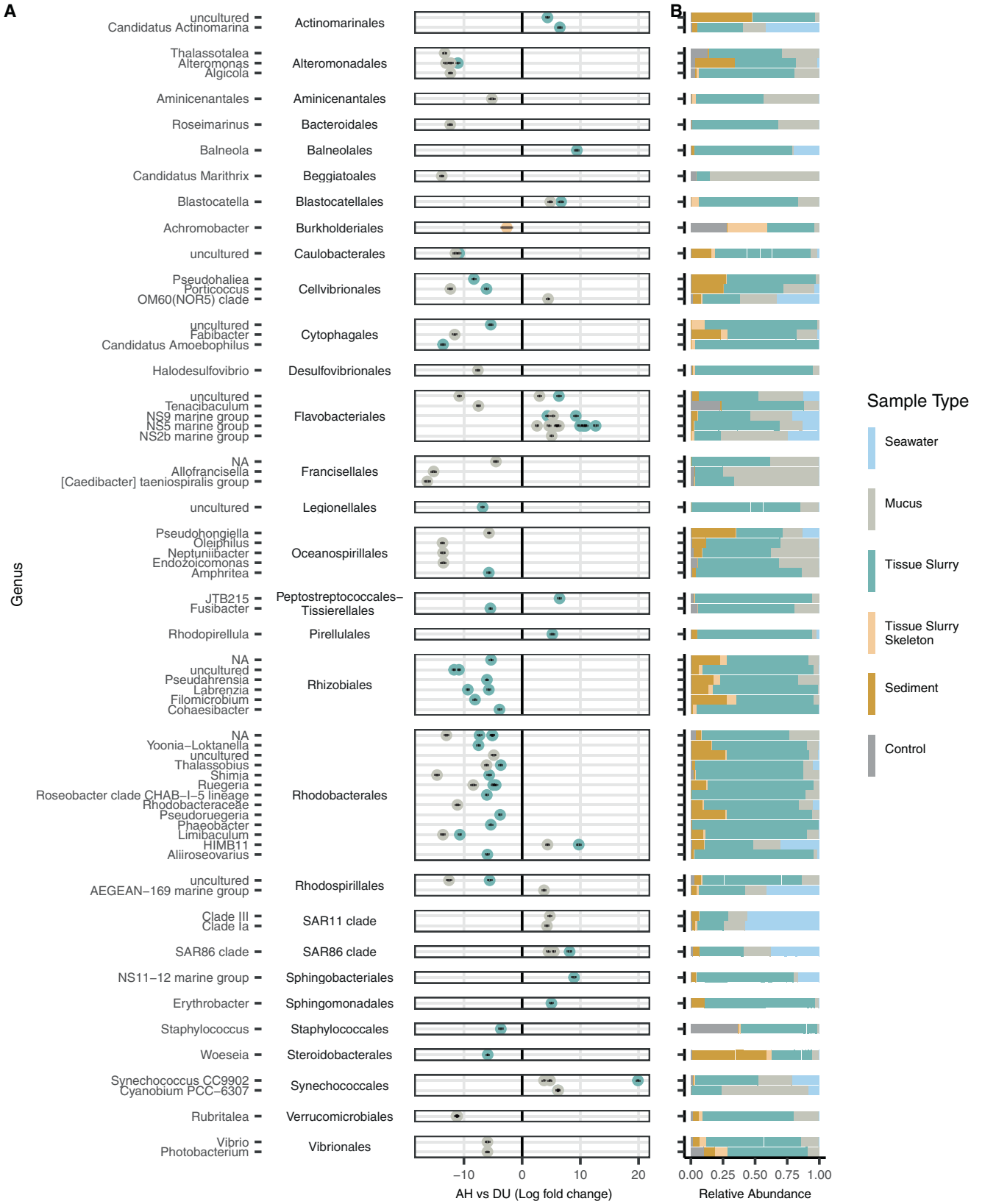

Fig. 5 Microbial amplicon sequence variants (ASVs) associated with unaffected areas on diseased colonies (DU). Differential abundances between (**A**) apparently healthy (AH) vs DU. The *y* axis depicts ASVs grouped by genus and then by order. Only ASVs with a *P*adj < 0.001, W statistic >90, and a log-fold change <−1.5 and >1.5 were visualized. Coral compartments (i.e., mucus, tissue slurry, and tissue slurry skeleton) were included and *Acropora* spp. were excluded from this analysis. **B** The relative abundance of taxa enriched in AH and DU by sample type, which includes laboratory controls ("Control") encompassing field, lab, kit, and mock communities.

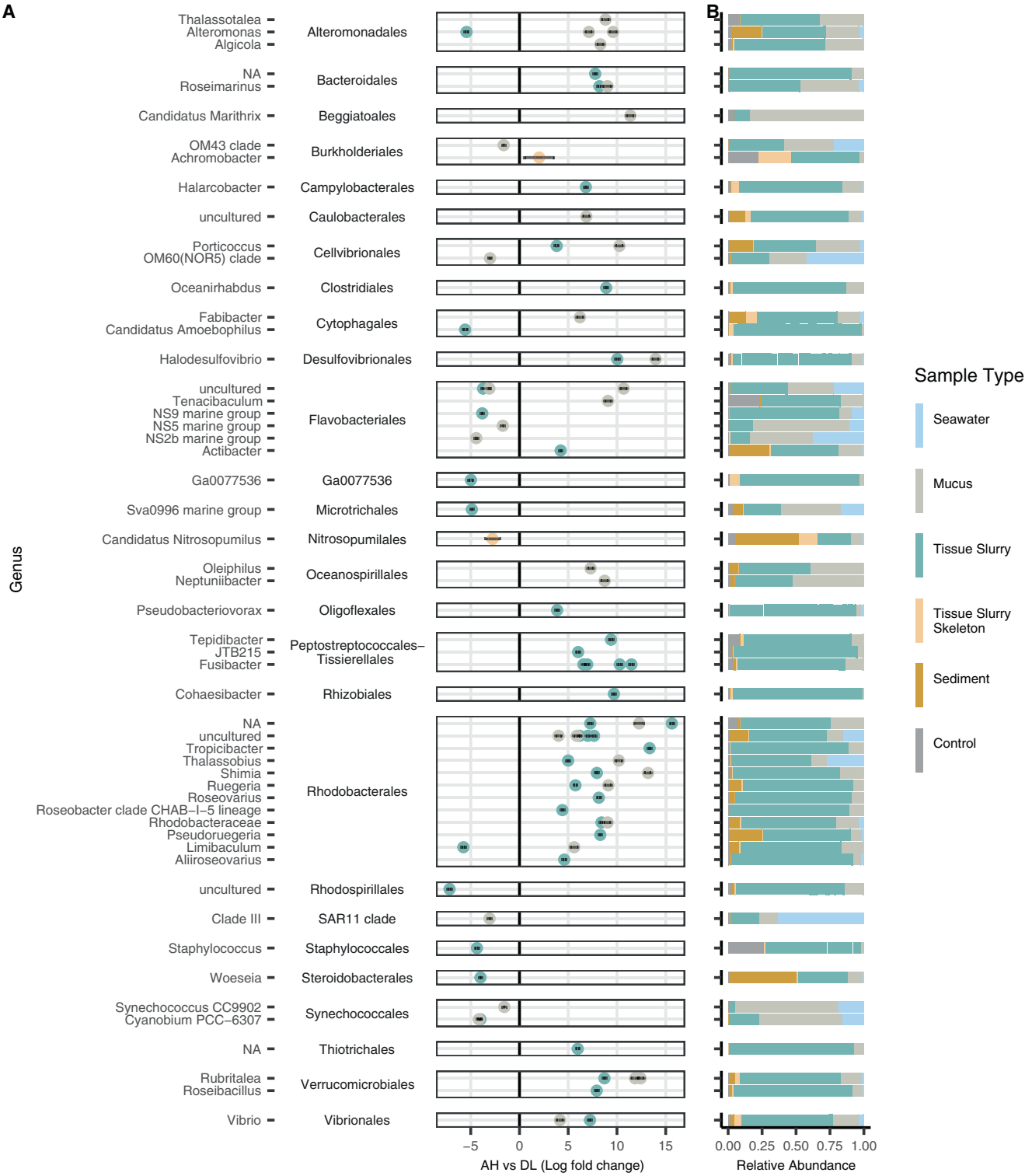

Fig. 6 Microbial amplicon sequence variants (ASVs) associated with lesions on diseased colonies (DL). Differential abundances between (**A**) apparently healthy (AH) vs DL. The *y* axis depicts ASVs grouped by genus and then by order. Only ASVs with a *P*adj < 0.001, W statistic >90, and a log-fold change <−1.5 and >1.5 were visualized. Coral compartments (i.e., mucus, tissue slurry, and tissue slurry skeleton) were included and *Acropora* spp. were excluded from this analysis. **B** The relative abundance of taxa enriched in AH and DL by sample type, which includes laboratory controls ("Control") encompassing field, lab, kit, and mock communities.

predictions. There was a total of 6307 differently abundant (*P*adj < 0.05) Kyoto Encyclopedia of Genes and Genomes (KEGG) pathways identified across AH ($n = 2482$), DU ($n = 1403$), and DL ($n = 2422$). Of the top ten KEGG pathways, three were enriched in DU and six in DL (Supplementary Fig. 11A). The most enriched pathway in DU was 4-hydroxybutyrate dehydrogenase (effect size = 0.25), and in DL was phospholipase C/alpha-toxin (effect size = 0.97). A total of 392 differentially abundant MetaCyc

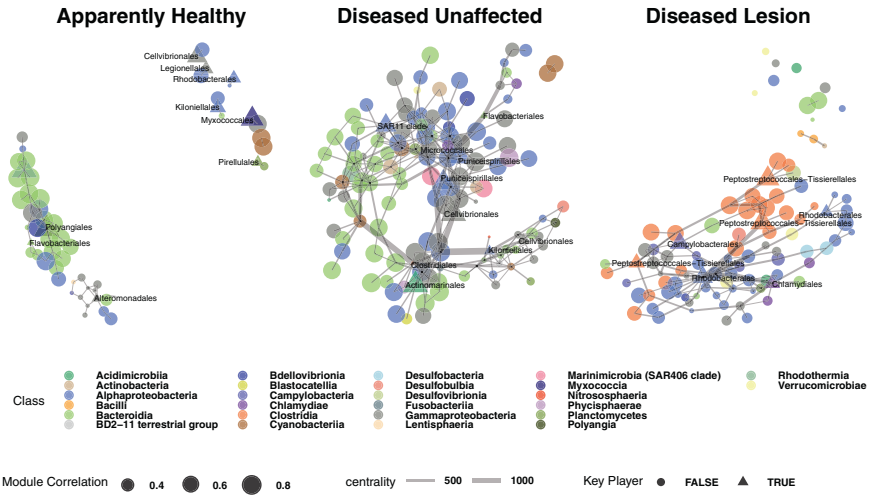

Fig. 7 Co-occurrence networks of bacteria from weighted correlation network analysis (WGCNA) modules (Supplementary Fig. 7) among apparently healthy colonies (AH), and unaffected (DU) and lesion (DL) areas on diseased colonies. The nodes represent amplicon sequence variants (ASV), which are sized by the ASV's correlation value to its respective module. A triangle and label of the bacteria order denote that a node is a "key player." The width of the edges corresponds to centrality, with thicker edges representing higher centrality. Samples from the three coral compartments (i.e., mucus, tissue slurry, and tissue slurry skeleton) were included in the analysis, and *Acropora* spp. samples were excluded from this analysis.

pathways were found across AH ($n = 148$), DU ($n = 104$), and DL ($n = 139$). Out of the top ten pathways, nine were enriched in DL and one in DU (Supplementary Fig. 11B). Biotin biosynthesis II was the most enriched pathway in DL (effect size = 0.80), and ADP-L-glycero-β-D-manno-heptose biosynthesis in DU (effect size = 0.05).

DISCUSSION

We used a crowdsourcing approach of both unpublished and published data to better understand stony coral tissue loss disease (SCTLD) across zones of disease spread (vulnerable, endemic, and epidemic), coral species, biomes (field vs aquaria), and studies to provide a more informed consensus on SCTLD community dynamics and associated bacteria. We identified potential changes to coral microbiomes based on the length of time the disease had been present in the area (i.e., epidemic vs endemic zones). We also found differences in alpha and beta-diversity by coral disease state: apparently healthy colonies (AH), and unaffected areas (DU) and lesions (DL) on diseased colonies. Furthermore, DU and DL showed unique sets of enriched bacteria, with DL microbiomes particularly structured by Rhodobacterales and Peptostreptococcales–Tissierellales interactions.

Apparently, healthy field-sourced coral microbiome composition differed among SCTLD zones

To understand if SCTLD alters the microbiome of visibly healthy corals on SCTLD-affected reefs, we examined AH corals within three disease zones: vulnerable, epidemic, and endemic. Although there were no differences in alpha-diversity and dispersion among zones, microbial beta-diversity and enriched microbial taxa were different among zones, as previously documented [11]. AH corals in the endemic and epidemic zones harbored more and higher relative abundances of SCTLD-associated microbes such as Alteromonadales, Vibrionales, Peptostreptococcales–Tissierellales, and Rhodobacterales compared to vulnerable reefs. This could potentially indicate that these corals were actively combating or showing signs of resistance to the disease. Flavobacteriales were the group with the most enriched taxa in endemic and epidemic AH corals, which is notable because Flavobacteriales were also detected in both DU and DL and are known to associate with corals under stressful conditions [39]. As AH corals showed no outward signs of lesions, members of Flavobacteriales may represent initial members of the SCTLD microbiome. However, a better understanding of the specific species/strains or genes expressed by Flavobacteriales present in both healthy and diseased corals may explain their enrichment in different health states, as Flavobacteriales was also found in AH corals from the vulnerable zone.

SCTLD aquaria studies may change microbial dynamics compared to field studies

We found that both biomes (aquaria and field) had distinct microbial compositions, which has been reported previously [40]. Despite this, we detected a microbial composition shift in disease states in both biomes. However, there were notable differences in the relative abundances of certain taxa between biomes. For example, while Rhodobacterales were dominant members in both biomes, they were found at higher relative abundances in aquaria compared to field samples. Because Rhodobacterales are primary surface colonizers in marine waters, including surfaces such as glass [41], aquarium environments may provide conditions that particularly enrich Rhodobacterales over other bacterial taxa. In addition, aquaria showed high relative abundances of Cytophagales in AH and DL, but this taxon was not a top abundant order in field samples. An aquaria coral challenge study with *Vibrio coralliilyticus* also showed an enrichment of both Rhodobacterales and Cytophagales [42], further indicating that these two bacteria may favor aquarium conditions, perhaps because there is a higher concentration of nutrients that attract these taxa in a more enclosed environment. Interestingly, Peptostreptococcales–Tissierellales, a bacterial group that appears to be important within SCTLD lesions, was present at similar relative abundances in DL in both biomes and thus may be less susceptible to laboratory artifacts, perhaps because this taxon has a more specialized niche (low or no oxygen environments) compared to Rhodobacterales, which are facultative anaerobes and can thrive in more diverse environments.

Notably, there were two aquaria experiments designed to limit the 'microbial background noise' from the field by using sterilized seawater [27] or sterilized sediment [12] and then incubating the chosen medium with healthy or diseased corals. The resulting bacterial communities from the incubated seawater and sediment clustered with aquaria coral samples rather than with field seawater and sediment samples, and show that these inoculums likely take

on the host microbial community. While field sediment and seawater samples showed distinct community separation from field coral samples, these samples still showed enrichment of some ASVs found in field DU and DL tissues, indicating potential transfer of microbes between diseased corals and their environment, which may result in the continued transmission of SCTLD [11, 12, 27].

Unaffected tissues on diseased colonies (DU) were enriched with Flavobacteriales and Synechococcales

This meta-analysis provides a comprehensive list of important microbial taxa in SCTLD across three coral compartments (mucus, tissue slurry, and tissue slurry skeleton) and three disease states (AH, DU, and DL). DU areas on coral colonies are of interest as they may represent an initial disturbance from SCTLD to the microbial community with potentially fewer secondary and saprophytic bacteria. It is unknown if SCTLD is a localized or systemic condition, but histological studies have found internal SCTLD lesions in DU tissue prior to lesion formation on the colony surface [1, 21]. We found that DU samples had the highest alpha-diversity and a distinct microbial composition, further suggesting that SCTLD also causes disruptions in the microbiome prior to surface lesion formation. Compared to AH, DU becomes particularly enriched with Flavobacteriales (class Bacteroidia) and Synechococcales (class Cyanophyceae), and these taxa formed strong connections to the class Alphaproteobacteria from the orders SAR11 and Rhodobacterales. Both SAR11 and Rhodobacterales respond strongly to dimethylsulphoniopropionate (DMSP), which is released by the coral and its symbiotic algae [43]. Stressed corals are known to release more DMSP than healthy ones [44, 45] and diseased corals may therefore be providing more favorable energy sources of sulfur and carbon and/or may act as a chemoattractant [45] to SAR11 and Rhodobacterales [44] in DU corals. SAR11 interactions may be particularly important in the mucus, where it was enriched, possibly due to exchange with the surrounding seawater, which also had high relative proportions of SAR11.

Of note, the increase in DU alpha-diversity could be partly driven by the lack of standardization of DU samples. One study collected DU samples from colonies in which DL tissues were treated with antibiotics ($n = 26$), potentially disrupting the DU microbiome [46]. The remaining studies consistently sampled DL at the lesion margin, but the DU samples varied in distance collected from the lesion. This may be driving the diversity detected, as the DU microbial community is known to change with distance from the lesion, with samples closest to the lesion possessing more SCTLD-associated taxa than those farther away [15]. A standardized definition of DU should be employed to maximize the utility of these samples. Regardless, the majority of DU-enriched taxa are likely not primary pathogens, but could be indicators of stressed corals. Some corals preferentially prey on Synechococcus as a nutritional source to recover from heat stress and bleaching [47–49] and may also use this mechanism under a diseased state. The majority of DU-enriched taxa were also found in the *Acropora* spp. rapid tissue loss (RTL) study. However, one Blastocatellales and Peptostreptococcales–Tissierellales ASV each were not found in the RTL study but were prevalent in 73% of the SCTLD studies, and therefore could be specific to SCTLD. Although these two ASVs have a 100% sequence similarity to bacteria found within black band disease (accession MH341639; [50]), and a paling necrosis study (GU200211.1; [51], respectively, the studies took place outside of the Caribbean, and thus the ASVs could belong to bacteria newly introduced to the area or not have been detected in previous studies because they were present at low abundance thresholds.

Rhodobacterales and Peptostreptococcales–Tissierellales were key structural components of microbial interactions in disease lesions (DL)

There was no clear transition from AH to DU to DL in alpha-diversity, and AH and DL alpha-diversity values were similar. It may be difficult to capture a general microbial alpha-diversity response to SCTLD across coral species, as alpha-diversity values are highly species-specific [26]. However, there were differences in microbial composition between AH and DL. In DL, the microbial community transitioned into an enrichment of Rhodobacterales and Peptostreptococcales–Tissierellales, which belong to the classes Alphaproteobacteria and Clostridia, respectively. Clostridia are anaerobic [52] and while Rhodobacterales are generally aerobic [53] they can thrive in anoxic conditions [54]. This suggests that as the disease state transitions from DU to DL, the lesion may progress to more anoxic conditions, as seen in black band disease [55]. However, the presence of Clostridia in DU samples suggests that prolonged anoxic conditions may be present prior to surface lesion appearance and decay on the coral; indeed, internal lesions within the basal body wall of the coral tissue, along the skeleton, have been observed in DU samples using light microscopy [1]. Presently, it cannot be determined if the shift to more anoxic conditions is a result of actions by the bacteria or if their enrichment is based on the shifting lesion environment [56]. Nonetheless, these two classes showed the highest connectivity and presence in the network analysis.

Across SCTLD microbiome studies, Rhodobacterales has been reported as highly abundant in all except one [24], and while Peptostreptococcales–Tissierellales has been found enriched in some studies [15, 16, 25, 26], Clostridia has been significantly enriched in all of them [11, 15, 16, 22, 24–27]. Rhodobacterales may be more generally associated with coral diseases, as many of the taxa associated with SCTLD were also found in the *Acropora* spp. RTL study and were found at relatively high abundances in sediment and seawater in the vulnerable zone. Rhodobacterales are generally abundant on coral reefs and may switch from commensals to pathogens when carbon sources change [57], such as when DMSP increases in stressed coral. Rhodobacterales specifically may be triggered to become a pathogen and activate virulence pathways such as the ferrous iron transporter (FeoB) pathway, which has been found in the genomes of Rhodobacterales from DL [22].

In contrast, Peptostreptococcales–Tissierellales were not as ubiquitous as Rhodobacterales. For example, these taxa were not found in RTL samples and a BLAST search of these ASVs showed that only one had 100% similarity to a sequence in the database, from a study that examined soil polluted by crude oil [55]. The rest were less than 94.31% similar to the NCBI 16S rRNA database, and these taxa were absent or at low relative abundances in vulnerable reefs, suggesting these taxa may be unique to SCTLD. Analysis of inferred functional traits showed that Clostridia taxa may have important roles in lesion progression through pathways such as phospholipase C/alpha-toxin, a toxin found in Clostridia such as *Clostridium perfringens* [58], and a top pathway predicted in DL in this study. Phospholipase C/alpha-toxin is a metalloenzyme that depends on zinc ions, which through lipid signaling degrades eukaryotic cell membranes and potentially causes necrosis [58]. Thus, Peptostreptococcales–Tissierellales could be contributing to tissue loss in SCTLD via an alpha-toxin by degrading coral and Symbiodiniaceae cells. However, an assembled genome of Peptostreptococcales–Tissierellales will be needed to confirm this functional gene prediction. Overall, the high network connectivity and inferred functional potential of toxin production suggest that Clostridia may have a particularly important role in SCTLD bacterial interactions and lesion progression. Therefore, promising future directions for SCTLD microbiome research could include developing enrichment media for Clostridia [59] and then conducting knockout gene studies of alpha-toxin genes [60].

Future SCTLD studies may consider sampling less-studied coral species

In this meta-analysis, only half of the coral species impacted by this disease were evaluated [2]. While we found consistent

bacterial enrichment between analyses with and without the two most frequently sampled coral species, coral species was found to be the main factor driving microbial community structure. Therefore, analyzing representatives of all susceptible coral species could be especially important in further narrowing down the microbial taxa specific to SCTLD. Future studies could consider including coral species with no or low sampling representation in their permits to enable opportunistic sampling, which when pooled together in a collaborative analysis such as this, may yield meaningful results.

CONCLUSIONS

This is the largest microbiome meta-analysis ever conducted on a coral disease. We found differences in the microbiomes of apparently healthy (AH) corals between SCTLD zones (vulnerable, endemic, and epidemic). In endemic and epidemic zones, AH corals may have acquired SCTLD-associated bacteria, potentially representing a compromised health state or resistance. We also identified that dominant taxa varied depending on whether the samples were collected away from the lesion (DU) or near the lesion (DL) on a colony with SCTLD. In DU samples, Flavobacteriales and Synechococcales were the dominant taxa, but in DL Rhodobacterales and Peptostreptococcales–Tissierellales were dominant and were key taxa in structuring microbial networks. This indicates that there is a shift of dominant bacterial taxa during disease progression and implies the lesion tissue may become anoxic. Specifically, during lesion progression, Peptostreptococcales–Tissierellales may be involved in tissue loss by lysing coral and symbiont cells through the phospholipase C/alpha-toxin pathway. Peptostreptococcales–Tissierellales taxa also appear to be more specifically associated with SCTLD and not a coral disease generalists, as some of the ASVs found here have not been reported in other coral diseases and were not abundant in vulnerable zones.

Our findings convey the need to focus on the transition of bacterial taxa from DU to DL and on characterizing the role of Peptostreptococcales–Tissierellales in lesion progression. A key aspect of this future work could be the inclusion of a wider assortment of coral species and compartments to better clarify the mechanisms of SCTLD. In addition, more holistic studies are needed to understand SCTLD. Our results suggest that the bacterial community may be involved in SCTLD, but other members of the holobiont (i.e., viruses and Symbiodiniaceae) may contribute to lesion progression. Combining multiple methods such as culturing, metagenomics, metatranscriptomics, and microscopy could help better clarify the microbial disease dynamics in SCTLD.

METHODS

Obtaining studies

To acquire small subunit (SSU) 16S rRNA datasets for this meta-analysis, an email was sent on July 14, 2020, and July 23, 2020, to the hosts of the coral-list listserv and the SCTLD Disease Advisory Committee (DAC) email list, respectively, requesting scientists to share unpublished SCTLD-associated microbiome datasets. In addition, to allow for comparisons of microbiomes between a past Caribbean coral disease to the novel SCTLD outbreak, a rapid tissue loss (RTL) disease study in *Acropora palmata* (APAL) and *Acropora cervicornis* (ACER) comprising apparently healthy (AH) samples, inoculated AH samples, and inoculated diseased samples [61], also was included in some analyses. This particular study was selected because *Acropora* spp. reportedly are not susceptible to SCTLD and the study used V4 primers [3]. In total, 17 studies were analyzed, 16 from SCTLD and one from an *Acropora* spp. RTL study (Supplementary Table 1).

Study authors were requested to complete a preformatted metadata file to facilitate comparisons of data across studies. Requested metadata included sample handling information (e.g., source laboratory, and sample collector) and ecological information (e.g., source reef name, coordinates, zone, water temperature, and coral colony measurements). SCTLD zones included vulnerable (i.e., locations where the disease had not been observed/reported), endemic (i.e., locations where the initial outbreak of the disease had moved through and no or few active lesions were observed on colonies), and epidemic (i.e., locations where the outbreak was active and prevalent across colonies of multiple species). Invasion zone sites, where the disease was newly arrived but not yet prevalent, were grouped within the epidemic zone for consistency across studies and simplicity of analysis. Some metadata required standardization of units and not all metadata were available across all studies. However, in all field-collected samples, all sampling dates and site information were available, enabling the completion of SCTLD disease zone metadata for Florida studies by referencing the Coral Reef Evaluation and Monitoring Project, Disturbance Response Monitoring, and SCTLD boundary reconnaissance databases. For USVI, zones were assigned based on the USVI Department of Planning and Natural Resources SCTLD database (https://dpnr.vi.gov/czm/sctld/).

Bioinformatics to process sequence data

Each sequencing run was imported to QIIME2-2022.2 [62, 63] and processed individually. The datasets were divided into two distinct pipelines: (1) data that targeted the 16S rRNA gene V4 region of Bacteria and/or Archaea and (2) data that targeted the V3–V4 region of Bacteria and/or Archaea. For V4 datasets, the data were processed with cut-adapt to remove sequencing primers corresponding to the respective study [64]. In total, three 515F primers that targeted the V4 region of the 16S rRNA gene were used across studies (5′-GTGCCAGCMGCCGCGGTAA-3′ ($n = 1033$) [31], 5′-GTGYCAGCMGCCGCGGTAA-3′ ($n = 1219$) [33], and 5′-ACACTGACGACATGGTTCTACAGTGCCAGCMGCCGCGGTAA-3′, ($n = 79$) [31, 32]; Supplementary Table 1). Next, the data were processed with DADA2 for quality control and denoising using a max error rate of three [65]. Although all runs were paired-end reads, the V4 samples were processed as single-end reads and the forward reads were truncated at 130 base pairs (bp) with the DADA2 program. The error rates, truncation, and single-end options were selected based on the quality and sequence length (Supplementary Table 1) of the lowest-quality reads across all datasets. The two V3–V4 datasets ($n = 31$ samples) were processed with the cut-adapt program, which was used to select forward sequences that contained sequences similar to the 515F primers used in the V4 studies. The forward primer 515FY [33] was used as the target sequence using a 0.4 error rate to allow for some differences in bases. The selected sequences were then processed with DADA2 and truncated at 240 bps with a max error rate of one. After, if studies had multiple Illumina sequencer runs, they were first merged together, and then all studies were merged into one count table and sequence file. The vsearch cluster-features-de-novo function was then used to cluster the data by 99% similarity [66]. The classify-consensus-vsearch option was then used for taxonomy assignments with the SILVA-138-99 database [67]. The data were then filtered to remove mitochondria and chloroplast reads. All analyses were conducted at the ASV level.

Alpha-diversity

Shannon diversity metrics were generated with the phyloseq function rarefy_even_depth with option replace = TRUE, and a minimum sequence depth for a sample of 1000. Prior to rarefaction, taxa with a sum of zero across the subsetted data were removed. Two sets of alpha-diversity analyses were run: [1] evaluated differences across the three zones (vulnerable, endemic, and epidemic) in field-sourced apparently healthy (AH) corals, and [2] evaluated differences across disease states (AH, unaffected tissue [DU], and lesion tissue [DL] on a diseased colony) in SCTLD-susceptible corals (i.e., without *Acropora* spp.). Significance was tested with linear mixed models with the R packages lme4 v1.1.21 [68], and emmeans v1.4.3.1 [69], and Tukey's HSD was used for pairwise comparisons. For zones and disease states, coral species was used as a random effect.

Beta-diversity

The data were imported into R v4.0.5 and converted into a phyloseq object [70]. ASVs were removed if they were present less than four times in 20% of the samples. The filtered count table was transformed using centered log-ratio (CLR) with the package microbiome [71]. Beta-diversity was analyzed with the package VEGAN 2.5.4 [72] and the filtered CLR-transformed table. The function vegdist was used to generate dissimilarity indices with a Euclidean distance. To identify significant differences among groups, a Permutational Multivariate Analysis of Variance (PERMANOVA) was used with the function adonis2 with 999 permutations, using a

Euclidean distance. The function betadisper was used to calculate group dispersion, which was then tested for significance with the function Permutest.

Differences in beta-diversity for field samples were evaluated in apparently healthy (AH) corals across three zones (vulnerable, endemic, and epidemic). In addition, pairwise group comparison was assessed from betadisper output using the Tukey's HSD function. The PERMANOVA output was also tested for pairwise comparisons with the function pairwise.adonis and adjusted with a Bonferroni correction [73]. Furthermore, all samples (including *Acropora* spp., sediment, and seawater) were also evaluated for beta-diversity differences in primers, year of collection, biome (field and aquaria), studies, coral species, and sample type (seawater, mucus, tissue slurry, tissue slurry and skeleton, and sediment). These factors were also correlated to principal components (PCs) using the R package PCAtools 2.5.15, and the functions pca and eigencorplot were used to remove the lowest 10% of the variance and to correlate the data and test for significance, respectively.

SCTLD-susceptible coral samples (i.e., without *Acropora* spp., sediment, and seawater) were also evaluated for beta-diversity. Both biomes (aquaria or field) were examined together and also separately. The matrices were generated with QIIME2-2021.11 with the plugin DEICODE, which runs a robust Aitchison Distance—a method that is not influenced by zeros in the data [74]. Pairwise comparisons of dispersion and differences in microbial composition between groups were evaluated using the QIIME2-2021.11 diversity beta-group-significance function using either the permdisp or PERMANOVA method, respectively. DEICODE was also applied to the data without the two most prevalent corals species, *Orbicella faveolata* (OFAV) and *Montastraea cavernosa* (MCAV), to see if the same pattern was evident in disease states with and without these coral species.

Differential abundance analysis

The program Analysis of Compositions of Microbiomes with Bias Correction (ANCOM_BC) was used to identify differentially abundant microbial taxa [75]. ANCOM_BC was used with the global test option and the results were considered significant if the false discovery rate adjusted p-value (*P*adj) was <0.001 and if the W statistic was >90. Field-sourced AH samples were tested for differential abundance among zones (vulnerable, endemic, and epidemic), and SCTLD-susceptible coral samples (without *Acropora* spp.) were evaluated for differences in disease state (AH, DU, and DL). For SCTLD-susceptible corals, the data were parsed by the three coral compartments (mucus, tissue slurry, and tissue slurry skeleton). ANCOM_BC analyses were run for each compartment due to the relatively low sample size of tissue slurry skeleton samples compared to the two other compartment types. The taxa were further evaluated if they had a log-fold change between $-1.5<$ and >1.5. The ASVs that were significantly enriched were used to identify the relative abundance of the ASVs across sample types and zones. In addition, those enriched only in either DU or DL were used to identify the presence or absence of each ASV in coral species and study per biome. The same ANCOM_BC analysis was repeated without MCAV and OFAV to evaluate if the two dominant coral species in our meta-analysis were driving the enriched bacteria.

Network analysis

To identify ASVs that co-associate in AH, DU, and DL samples, CLR-transformed counts were used for weighted correlation network analysis (WGCNA) with the WGCNA 1.70-3R package [76]. The network was constructed unsigned with the following parameters: power = 3, minimum module size = 12, deep split = 2, and merged cut height = 0.25. The eigenvalues were correlated to AH, DU, and DL using Pearson correlation with the R function cor. The highest correlation in each disease state was then selected for network construction using the R package SpiecEasi 1.0.5 [77]. The network was then constructed as previously reported [11]. Briefly, the Stability Approach to Regularization Selection (StARS) [77] model was chosen along with the method Meinshausen–Bühlmann's neighborhood selection [78]. For StARS, 100 subsamples were used with a variability threshold of 10^{-3}. The centrality (node importance) was evaluated [79] using the functions centrality_degree (neighbors = the number of adjacent edges or neighbors) and centrality_edge_betweenness (centrality = the number of shortest paths going through an edge) [80]. The package influenceR 0.1.0. [81] selected important ASVs in each network and assigned the top "key players" [38], which were labeled with their respective orders.

Functional prediction profiles

To infer the functional potential of 16S rRNA gene data among AH, DU, and DL, the program Phylogenetic Investigation of Communities by Reconstruction of Unobserved States (PICRUSt2) was used in QIIME2-2021.11 [82]. Only SCTLD-susceptible corals were evaluated and only ASVs that were present in at least 100 samples were selected. The picrust2 full-pipeline was used with the hidden state set to "mp" and the placement tool to place sequences into a tree set to "epa-ng." The outputs were predicted metagenomes for Kyoto Encyclopedia of Genes and Genomes (KEGG [83]) orthologs and MetaCyc pathway [84] abundances. To assess the differential abundance of these outputs among disease states, the R package Maaslin2 was utilized [85]. For both KEGG and MetaCyc tests, data were log-transformed, a random effect was set to coral species, and the data were subsequently analyzed with a linear model. In the KEGG assessment, the minimum abundance = 0.05 and the minimum prevalence = 0.1. There were no minimums set for the MetaCyc test due to the lower number of pathways found in MetaCyc. The top 10 predicted pathways were selected based on values with the lowest *P*adj and effect sizes < -0.5 and >0.5. The top pathways were manually annotated on KEGG and MetaCyc websites.

DATA AVAILABILITY

Sequence data available on NCBI are listed in Supplementary Table 1. All other datasets are available upon request. The unfiltered ASV counts table, taxonomy table, ASV sequences, and code used to conduct this analysis are publicly available at https://github.com/srosales712/SCTLD_microbiome_meta_analysis.

REFERENCES

1. Landsberg JH, Kiryu Y, Peters EC, Wilson PW, Perry N, Waters Y, et al. Stony coral tissue loss disease in Florida is associated with disruption of host—Zooxanthellae physiology. Front Mar Sci. 2020;7:576013. https://doi.org/10.3389/fmars.2020.576013.
2. Case definition: stony coral tissue loss disease (SCTLD). https://floridadep.gov/sites/default/files/Copy%20of%20StonyCoralTissueLossDisease_CaseDefinition%20final%2010022018.pdf. Accessed 12 July, 2022.
3. Precht WF, Gintert BE, Robbart ML, Fura R, van Woesik R. Unprecedented disease-related coral mortality in southeastern Florida. Sci Rep. 2016;6. https://doi.org/10.1038/srep31374.
4. Miller M, Karazsia J, Groves CE, Griffin S, Moore T, Wilber P, et al. Detecting sedimentation impacts to coral reefs resulting from dredging the port of Miami, Florida USA. PeerJ. 2016;4:e2711. https://doi.org/10.7717/peerj.2711.
5. Walton CJ, Hayes NK, Gilliam DS. Impacts of a regional, multi-year, multi-species coral disease outbreak in southeast Florida. Front Mar Sci. 2018;5. https://doi.org/10.3389/fmars.2018.00323.
6. Gintert BE, Precht WF, Fura R, Rogers K, Rice M, Precht LL, et al. Regional coral disease outbreak overwhelms impacts from a local dredge project. Environ Monitor Assess. 2019;191. https://doi.org/10.1007/s10661-019-7767-7.
7. Alvarez-Filip L, Estrada-Saldívar N, Pérez-Cervantes E, Molina-Hernández A, González-Barrios FJ. A rapid spread of the stony coral tissue loss disease outbreak in the Mexican Caribbean. PeerJ. 2019;7:e8069. https://doi.org/10.7717/peerj.8069.
8. Alvarez-Filip L, González-Barrios FJ, Pérez-Cervantes E, Molina-Hernández A, Estrada-Saldívar N. Stony coral tissue loss disease decimated Caribbean coral populations and reshaped reef functionality. Commun Biol. 2022;5:440. https://doi.org/10.1038/s42003-022-03398-6.
9. Williams SD, Walter CS, Muller EM. Fine scale temporal and spatial dynamics of the stony coral tissue loss disease outbreak within the lower Florida keys. Front Mar Sci. 2021;8:631776. https://doi.org/10.3389/fmars.2021.631776.
10. Hayes NK, Walton CJ, Gilliam DS. Tissue loss disease outbreak significantly alters the Southeast Florida stony coral assemblage. Front Mar Sci. 2022;9:975894. https://doi.org/10.3389/fmars.2022.975894.
11. Rosales SM, Clark AS, Huebner LK, Ruzicka RR, Muller EM. Rhodobacterales and Rhizobiales are associated with stony coral tissue loss disease and its suspected sources of transmission. Front Microbiol. 2020;11. https://doi.org/10.3389/fmicb.2020.00681.
12. Studivan MS, Rossin AM, Rubin E, Soderberg N, Holstein DM, Enochs IC. Reef sediments can act as a stony coral tissue loss disease vector. Front Mar Sci. 2022;8:815698. https://doi.org/10.3389/fmars.2021.815698.
13. Work TM, Weatherby TM, Landsberg JH, Kiryu Y, Cook SM, Peters EC. Viral-like particles are associated with endosymbiont pathology in Florida corals affected by stony coral tissue loss disease. Front Mar Sci. 2021;8:750658. https://doi.org/10.3389/fmars.2021.750658.

14. Veglia AJ, Beavers K, Van Buren EW, Meiling SS, Muller EM, Smith TB, et al. Alphaflexivirus genomes in stony coral tissue loss disease-affected, disease-exposed, and disease-unexposed coral colonies in the U.S. Virgin Islands. Microbiol Resour Announc. 2022;11:e01199-21. https://doi.org/10.1128/mra.01199-21.
15. Meyer JL, Castellanos-Gell J, Aeby GS, Häse CC, Ushijima B, Paul VJ. Microbial community shifts associated with the ongoing stony coral tissue loss disease outbreak on the Florida reef tract. Front Microbiol. 2019;10. https://doi.org/10.3389/fmicb.2019.02244.
16. Huntley N, Brandt ME, Becker CC, Miller CA, Meiling SS, Correa AMS, et al. Experimental transmission of stony coral tissue loss disease results in differential microbial responses within coral mucus and tissue. ISME Commun. 2022;2:46. https://doi.org/10.1038/s43705-022-00126-3.
17. Muller EM, Sartor C, Alcaraz NI, van Woesik R. Spatial epidemiology of the stony-coral-tissue-loss disease in Florida. Front Mar Sci. 2020;7:163. https://doi.org/10.3389/fmars.2020.00163.
18. Meiling S, Muller EM, Smith TB, Brandt ME. 3D photogrammetry reveals dynamics of stony coral tissue loss disease (SCTLD) lesion progression across a thermal stress event. Front Mar Sci. 2020;7:597643. https://doi.org/10.3389/fmars.2020.597643.
19. Aeby GS, Ushijima B, Campbell JE, Jones S, Williams GJ, Meyer JL, et al. Pathogenesis of a tissue loss disease affecting multiple species of corals along the Florida reef tract. Front Mar Sci. 2019;6. https://doi.org/10.3389/fmars.2019.00678.
20. Dobbelaere T, Muller EM, Gramer LJ, Holstein DM, Hanert E. Coupled epidemiohydrodynamic modeling to understand the spread of a deadly coral disease in Florida. Front Mar Sci. 2020;7:591881. https://doi.org/10.3389/fmars.2020.591881.
21. Eaton KR, Landsberg JH, Kiryu Y, Peters EC, Muller EM. Measuring stony coral tissue loss disease induction and lesion progression within two intermediately susceptible species, *Montastraea cavernosa* and *Orbicella faveolata*. Front Mar Sci. 2021;8:717265. https://doi.org/10.3389/fmars.2021.717265.
22. Rosales SM, Huebner LK, Clark AS, McMinds R, Ruzicka RR, Muller EM. Bacterial metabolic potential and micro-eukaryotes enriched in stony coral tissue loss disease lesions. Front Mar Sci. 2022;8:776859. https://doi.org/10.3389/fmars.2021.776859.
23. Iwanowicz DD, Schill WB, Woodley CM, Bruckner A, Neely K, Briggs KM. Exploring the stony coral tissue loss disease bacterial pathobiome. 2020. https://doi.org/10.1101/2020.05.27.120469. Accessed 22 October 2020.
24. Thome PE, Rivera-Ortega J, Rodríguez-Villalobos JC, Cerqueda-García D, Guzmán-Urieta EO, García-Maldonado JQ, et al. Local dynamics of a white syndrome outbreak and changes in the microbial community associated with colonies of the scleractinian brain coral *Pseudodiploria strigosa*. PeerJ. 2021;9:e10695. https://doi.org/10.7717/peerj.10695.
25. Becker CC, Brandt M, Miller CA, Apprill A. Microbial bioindicators of stony coral tissue loss disease identified in corals and overlying waters using a rapid field-based sequencing approach. Environ Microbiol. 2021;1462-2920:15718 https://doi.org/10.1111/1462-2920.15718.
26. Clark AS, Williams SD, Maxwell K, Rosales SM, Huebner LK, Landsberg JH, et al. Characterization of the microbiome of corals with stony coral tissue loss disease along Florida's coral reef. Microorganisms. 2021;9:2181. https://doi.org/10.3390/microorganisms9112181.
27. Evans JS, Paul VJ, Ushijima B, Kellogg CA. Combining tangential flow filtration and size fractionation of mesocosm water as a method for the investigation of waterborne coral diseases. Biol Methods Protoc. 2022;7:bpac007. https://doi.org/10.1093/biomethods/bpac007.
28. Neely KL, Macaulay KA, Hower EK, Dobler MA. Effectiveness of topical antibiotics in treating corals affected by stony coral tissue loss disease. PeerJ. 2020;8:e9289. https://doi.org/10.7717/peerj.9289.
29. Walker BK, Turner NR, Noren HKG, Buckley SF, Pitts KA. Optimizing stony coral tissue loss disease (SCTLD) intervention treatments on *Montastraea cavernosa* in an endemic zone. Front Mar Sci. 2021;8:666224. https://doi.org/10.3389/fmars.2021.666224.
30. The Microbiome Quality Control Project Consortium, Sinha R, Abu-Ali G, Vogtmann E, Fodor AA, Ren B, et al. Assessment of variation in microbial community amplicon sequencing by the Microbiome Quality Control (MBQC) project consortium. Nat Biotechnol. 2017;35:1077–86. https://doi.org/10.1038/nbt.3981.
31. Caporaso JG, Lauber CL, Walters WA, Berg-Lyons D, Lozupone CA, Turnbaugh PJ, et al. Global patterns of 16S rRNA diversity at a depth of millions of sequences per sample. Proc Natl Acad Sci USA. 2011;108:4516–22. https://doi.org/10.1073/pnas.1000080107.
32. Green SJ, Venkatramanan R, Naqib A. Deconstructing the polymerase chain reaction: understanding and correcting bias associated with primer degeneracies and primer-template mismatches. PLOS ONE. 2015;10:e0128122. https://doi.org/10.1371/journal.pone.0128122.
33. Parada AE, Needham DM, Fuhrman JA. Every base matters: assessing small subunit rRNA primers for marine microbiomes with mock communities, time series and global field samples: primers for marine microbiome studies. Environ Microbiol. 2016;18:1403–14. https://doi.org/10.1111/1462-2920.13023.
34. Apprill A, McNally S, Parsons R, Weber L. Minor revision to V4 region SSU rRNA 806R gene primer greatly increases detection of SAR11 bacterioplankton. Aquatic Microbial Ecol. 2015;75:129–37. https://doi.org/10.3354/ame01753.
35. Herlemann DP, Labrenz M, Jürgens K, Bertilsson S, Waniek JJ, Andersson AF. Transitions in bacterial communities along the 2000 km salinity gradient of the Baltic Sea. ISME J. 2011;5:1571–9. https://doi.org/10.1038/ismej.2011.41.
36. Takai K, Horikoshi K. Rapid detection and quantification of members of the archaeal community by quantitative PCR using fluorogenic probes. Appl Environ Microbiol. 2000;66:5066–72. https://doi.org/10.1128/AEM.66.11.5066-5072.2000.
37. Salter SJ, Cox MJ, Turek EM, Calus ST, Cookson WO, Moffatt MF, et al. Reagent and laboratory contamination can critically impact sequence-based microbiome analyses. BMC Biol. 2014;12:87. https://doi.org/10.1186/s12915-014-0087-z.
38. Borgatti SP. Identifying sets of key players in a social network. Comput Math Organ Theory. 2006;12:21–34. https://doi.org/10.1007/s10588-006-7084-x.
39. McDevitt-Irwin JM, Baum JK, Garren M, Vega Thurber RL. Responses of coral-associated bacterial communities to local and global stressors. Front Mar Sci. 2017;4. https://doi.org/10.3389/fmars.2017.00262.
40. Galand PE, Chapron L, Meistertzheim AL, Peru E, Lartaud F. The effect of captivity on the dynamics of active bacterial communities differs between two deep-sea coral species. Front Microbiol. 2018;9:2565. https://doi.org/10.3389/fmicb.2018.02565.
41. Dang H, Li T, Chen M, Huang G. Cross-ocean distribution of rhodobacterales bacteria as primary surface colonizers in temperate coastal marine waters. Appl Environ Microbiol. 2008;74:52–60. https://doi.org/10.1128/AEM.01400-07.
42. Welsh RM, Rosales SM, Zaneveld JR, Payet JP, McMinds R, Hubbs SL, et al. Alien vs. predator: bacterial challenge alters coral microbiomes unless controlled by *Halobacteriovorax* predators. PeerJ. 2017;5:e3315. https://doi.org/10.7717/peerj.3315.
43. Tripp HJ, Kitner JB, Schwalbach MS, Dacey JWH, Wilhelm LJ, Giovannoni SJ. SAR11 marine bacteria require exogenous reduced sulphur for growth. Nature. 2008;452:741–4. https://doi.org/10.1038/nature06776.
44. Raina JB, Dinsdale EA, Willis BL, Bourne DG. Do the organic sulfur compounds DMSP and DMS drive coral microbial associations? Trend Microbiol. 2010;18:101–8. https://doi.org/10.1016/j.tim.2009.12.002.
45. Garren M, Son K, Raina JB, Rusconi R, Menolascina F, Shapiro OH, et al. A bacterial pathogen uses dimethylsulfoniopropionate as a cue to target heat-stressed corals. ISME J. 2014;8:999–1007. https://doi.org/10.1038/ismej.2013.210.
46. Shilling EN, Combs IR, Voss JD. Assessing the effectiveness of two intervention methods for stony coral tissue loss disease on *Montastraea cavernosa*. Sci Rep. 2021;11:8566. https://doi.org/10.1038/s41598-021-86926-4.
47. McNally SP, Parsons RJ, Santoro AE, Apprill A. Multifaceted impacts of the stony coral *Porites astreoides* on picoplankton abundance and community composition. Limnol Oceanogr. 2017;62:217–34. https://doi.org/10.1002/lno.10389.
48. Meunier V, Bonnet S, Pernice M, Benavides M, Lorrain A, Grosso O, et al. Bleaching forces coral's heterotrophy on diazotrophs and Synechococcus. ISME J. 2019;13:2882–6. https://doi.org/10.1038/s41396-019-0456-2.
49. Hoadley KD, Hamilton M, Poirier CL, Choi CJ, Yung CM, Worden AZ. Selective uptake of pelagic microbial community members by Caribbean reef corals. App Environ Microbiol. 2021;87:e03175-20. https://doi.org/10.1128/AEM.03175-20.
50. Hadaidi G, Ziegler M, Shore-Maggio A, Jensen T, Aeby G, Voolstra CR. Ecological and molecular characterization of a coral black band disease outbreak in the Red Sea during a bleaching event. PeerJ. 2018;6:e5169. https://doi.org/10.7717/peerj.5169.
51. de Castro AP, Araújo SD, Reis AMM, Moura RL, Francini-Filho RB, Pappas G, et al. Bacterial community associated with healthy and diseased reef coral *Mussismilia hispida* from eastern Brazil. Microbial Ecol. 2010;59:658–67. https://doi.org/10.1007/s00248-010-9646-1.
52. Dürre P. Clostridia. eLS. 2015; 1–11. https://doi.org/10.1002/9780470015902.a0020370.pub2.
53. Pujalte MJ, Lucena T, Ruvira MA, Arahal DR, Macián MC. The Family Rhodobacteraceae. In: Rosenberg E, DeLong EF, Lory S, Stackebrandt E, Thompson F, editors. The Prokaryotes. Berlin, Heidelberg: Springer Berlin Heidelberg; 2014. p. 439–512.
54. Pohlner M, Dlugosch L, Wemheuer B, Mills H, Engelen B, Reese BK. The majority of active Rhodobacteraceae in marine sediments belong to uncultured genera: a molecular approach to link their distribution to environmental conditions. Front Microbiol. 2019;10:659. https://doi.org/10.3389/fmicb.2019.00659.
55. Carlton RG, Richardson LL. Oxygen and sulfide dynamics in a horizontally migrating cyanobacterial mat: black band disease of corals. FEMS Microbiol Ecol. 1995;18:155–62. https://doi.org/10.1111/j.1574-6941.1995.tb00173.x.
56. Hughes DJ, Raina JB, Nielsen DA, Suggett DJ, Kühl M. Disentangling compartment functions in sessile marine invertebrates. Trends Ecol Evol. 2022;S016953472200091X. https://doi.org/10.1016/j.tree.2022.04.008.
57. Cárdenas A, Neave MJ, Haroon MF, Pogoreutz C, Rädecker N, Wild C, et al. Excess labile carbon promotes the expression of virulence factors in coral reef bacterioplankton. ISME J. 2018;12:59–76. https://doi.org/10.1038/ismej.2017.142.

58. Urbina P, Collado MI, Alonso A, Goñi FM, Flores-Díaz M, Alape-Girón A, et al. Unexpected wide substrate specificity of *C. perfringens* α-toxin phospholipase C. Biochimica et Biophysica Acta (BBA) - Biomembranes. 2011;1808:2618–27. https://doi.org/10.1016/j.bbamem.2011.06.008.
59. Anwar Z, Regan SB, Linden J. Enrichment and detection of *Clostridium perfringens* toxinotypes in retail food samples. J Vis Exp. 2019:59931. https://doi.org/10.3791/59931.
60. Chen Y, McClane BA, Fisher DJ, Rood JI, Gupta P. Construction of an alpha toxin gene knockout mutant of *Clostridium perfringens* type A by use of a mobile group II intron. Appl Environ Microbiol. 2005;71:7542–7. https://doi.org/10.1128/AEM.71.11.7542-7547.2005.
61. Rosales SM, Miller MW, Williams DE, Traylor-Knowles N, Young B, Serrano XM. Microbiome differences in disease-resistant vs. susceptible Acropora corals subjected to disease challenge assays. Sci Rep. 2019;9. https://doi.org/10.1038/s41598-019-54855-y.
62. Bolyen E, Rideout JR, Dillon MR, Bokulich NA, Abnet C, Al-Ghalith GA, et al. QIIME 2: Reproducible, interactive, scalable, and extensible microbiome data science. PeerJ. 2018; https://doi.org/10.7287/peerj.preprints.27295v2.
63. Estaki M, Jiang L, Bokulich NA, McDonald D, González A, Kosciolek T, et al. QIIME 2 enables comprehensive end-to-end analysis of diverse microbiome data and comparative studies with publicly available data. Curr Protoc Bioinform. 2020;70. https://doi.org/10.1002/cpbi.100.
64. Martin M. Cutadapt removes adapter sequences from high-throughput sequencing reads. EMBnet.journal. 2011;17:10. https://doi.org/10.14806/ej.17.1.200.
65. Callahan BJ, McMurdie PJ, Rosen MJ, Han AW, Johnson AJA, Holmes SP. DADA2: high-resolution sample inference from Illumina amplicon data. Nat Methods. 2016;13:581–3. https://doi.org/10.1038/nmeth.3869.
66. Rognes T, Flouri T, Nichols B, Quince C, Mahé F. VSEARCH: a versatile open source tool for metagenomics. PeerJ. 2016;4:e2584 https://doi.org/10.7717/peerj.2584.
67. Quast C, Pruesse E, Yilmaz P, Gerken J, Schweer T, Yarza P, et al. The SILVA ribosomal RNA gene database project: improved data processing and web-based tools. Nucleic Acids Res. 2012;41:D590–D596. https://doi.org/10.1093/nar/gks1219.
68. Bates D, Mächler M, Bolker B, Walker S. Fitting linear mixed-effects models using lme4. J Stat Softw. 2015;67. https://doi.org/10.18637/jss.v067.i01.
69. Searle SR, Speed FM, Milliken GA. Population marginal means in the linear model: an alternative to least squares means. Am Stat. 1980;34:216–21. https://doi.org/10.1080/00031305.1980.10483031.
70. McMurdie PJ, Holmes S. phyloseq: an R package for reproducible interactive analysis and graphics of microbiome census data. PLoS ONE. 2013;8:e61217. https://doi.org/10.1371/journal.pone.0061217.
71. Lahti L, Shetty S. Tools for microbiome analysis in R. Microbiome package version. Bioconductor; 2017. http://microbiome.github.io/microbiome.
72. Dixon P. VEGAN, a package of R functions for community ecology. J Veget Sci. 2003;14:927–30. https://doi.org/10.1111/j.1654-1103.2003.tb02228.x.
73. Martinez A. pairwiseAdonis: pairwise multilevel comparison using adonis. 2019. https://github.com/pmartinezarbizu/pairwiseAdonis.
74. Martino C, Morton JT, Marotz CA, Thompson LR, Tripathi A, Knight R, et al. A novel sparse compositional technique reveals microbial perturbations. mSystems. 2019;4:e00016-19. https://doi.org/10.1128/mSystems.00016-19.
75. Lin H, Peddada SD. Analysis of compositions of microbiomes with bias correction. Nat Commun. 2020;11. https://doi.org/10.1038/s41467-020-17041-7.
76. Langfelder P, Horvath S. WGCNA: an R package for weighted correlation network analysis. BMC Bioinform. 2008;9:559 https://doi.org/10.1186/1471-2105-9-559.
77. Kurtz ZD, Müller CL, Miraldi ER, Littman DR, Blaser MJ, Bonneau RA. Sparse and compositionally robust inference of microbial ecological networks. PLOS Comput Biol. 2015;11:e1004226. https://doi.org/10.1371/journal.pcbi.1004226.
78. Meinshausen N, Bühlmann P. High-dimensional graphs and variable selection with the Lasso. Annal Stat. 2006;34:1436–62. https://doi.org/10.1214/009053606000000281.
79. Thomas LP. A tidy API for graph manipulation. 2019. https://github.com/thomasp85/tidygraph
80. Brandes U. A faster algorithm for betweenness centrality. J Math Sociol. 2001;25:163–77. https://doi.org/10.1080/0022250X.2001.9990249.
81. Simon J. influenceR: software tools to quantify structural importance of nodes in a network. 2015. https://github.com/rcc-uchicago/influenceR
82. Douglas GM, Maffei VJ, Zaneveld JR, Yurgel SN, Brown JR, Taylor CM, et al. PICRUSt2 for prediction of metagenome functions. Nat Biotechnol. 2020;38:685–8. https://doi.org/10.1038/s41587-020-0548-6.
83. Kanehisa M. KEGG: kyoto encyclopedia of genes and genomes. Nucleic Acids Res. 2000;28:27–30. https://doi.org/10.1093/nar/28.1.27.
84. Caspi R, Billington R, Keseler IM, Kothari A, Krummenacker M, Midford PE, et al. The MetaCyc database of metabolic pathways and enzymes—a 2019 update. Nucleic Acids Res. 2020;48:D445–53. https://doi.org/10.1093/nar/gkz862.
85. Mallick H, Rahnavard A, McIver LJ, Ma S, Zhang Y, Nguyen LH, et al. Multivariable association discovery in population-scale meta-omics studies. PLoS Comput Biol. 2021;17:e1009442. https://doi.org/10.1371/journal.pcbi.1009442.

ACKNOWLEDGEMENTS

Any use of trade, firm, or product names is for descriptive purposes only and does not imply endorsement by the U.S. Government. We would like to thank the Disease Advisory Committee Pathogen ID/Microbiome sub-team which spawned the "Sweet 16S" team that led to this paper. SMR was supported by the National Oceanic and Atmospheric Administration (NOAA) Office of Oceanic and Atmospheric Research (OAR) omics initiative. LKH was supported by the Environmental Protection Agency South Florida Initiative grants X7-00D66417-0 and X7-01D00820-0. JSE, CAK, and WBS were supported by the USGS Ecosystems Biological Threats & Invasive Species Research Program. AA was supported by National Science Foundation awards 1938112 and 2109622 and a NOAA OAR Cooperative Institutes award. EMM was supported by a Mote Eminent Scholarship. ENS and JDV were supported by Florida Department of Environmental Protection, Professional Association of Diving Instructors, and the Harbor Branch Oceanographic Institute Foundation.

AUTHOR CONTRIBUTIONS

SMR performed analysis and wrote the manuscript. LKH and JSM helped with writing the manuscript and helped curate metadata file. AA, ACK, AJB, ASC, CED, CAK, ENS, EMM, JDV, JLS, JMS, NEH, MM, MRL, and WBS provided unpublished sequence data and the preformatted metadata file. SMR, LKH, JSM, AA, ASC, CAK, EMM, JDC, JLM, JLS, JMS, and WBS conceived of this study, provided input on data analysis, and assisted with the interpretation of results. All authors edited the manuscript.

COMPETING INTERESTS

The authors declare no competing interests.

ADDITIONAL INFORMATION

Supplementary information The online version contains supplementary material available at https://doi.org/10.1038/s43705-023-00220-0.

Correspondence and requests for materials should be addressed to Stephanie M. Rosales.

Reprints and permission information is available at http://www.nature.com/reprints

Publisher's note Springer Nature remains neutral with regard to jurisdictional claims in published maps and institutional affiliations.